

Modeling of coastal erosion and sediment deposition during the 2004 Indian Ocean tsunami in Lhok Nga, Sumatra, Indonesia

Budianto Ontowirjo · Raphaël Paris · Akira Mano

Received: 27 April 2012 / Accepted: 12 October 2012 / Published online: 18 October 2012
© Springer Science+Business Media Dordrecht 2012

Abstract This study presents the results of numerical simulations of the 2004 Indian Ocean earthquake and tsunami in the Bay of Lhok Nga (northwestern coast of Sumatra, Indonesia) integrating sediment erosion and deposition. We investigate the transport of sediment both by suspension and by bedload under different scenarios of long breaking dispersive waves through a series of numerical experiments. The earthquake source model used by Koshimura et al. (Coast Eng J 51:243–273, 2008) with a 25-m dislocation better reproduces the wave travel time, flow depth and inundation area than the other models tested. The model reproduces realistically the pronounced coastal retreat in the northern part of Lhok Nga Bay (retreat ranging between 50 and 150 m), where Paris et al. (Geomorphology 104:59–72, 2009) estimated a mean retreat of 80 m. There is also a good agreement between the simulated area of coastal retreat (195,400 m²) and the field observations (203,200 m²). The simulation may underestimate the volume of tsunami deposits (611,700 m³ vs. 500,000–1,000,000 m³ estimated by Paris et al. (2009)). The model fully reproduces the observed thickness of tsunami deposits when considering both bedload and suspension, even if bedload transport dominates. Limitations are due to micro-scale topographic, anthropic features (which are not always represented by the DEM) and the amount of debris which may influence flow dynamics and sediment transport.

Keywords Tsunami · Dispersive wave · Sediment transport · Indian Ocean tsunami

B. Ontowirjo · R. Paris (✉)
Clermont Université, Université Blaise Pascal, BP 10448, 63000 Clermont-Ferrand, France
e-mail: R.Paris@opgc.univ-bpclermont.fr

B. Ontowirjo
CNRS, UMR 6042, GEOLAB, 63057 Clermont-Ferrand, France

R. Paris
CNRS, UMR 6524, Magmas et Volcans, 63038 Clermont-Ferrand, France

A. Mano
IRIDeS, International Research Institute of Natural Disaster, Tohoku University, 6-6-1110, Aoba,
Sendai 980-8579, Japan

1 Introduction

Reconstructing the flow depth, velocity and inundation distance of a tsunami after its deposits is still difficult and represents a challenging topic for improving tsunami hazard management. Main limitations are related to (1) the great variability of tsunami sandy sheets deposited on land, the sediment source and the topography controlling many aspects of the transport and deposition (e.g., Umitsu et al. 2007; Choowong et al. 2008; Morton et al. 2008), and (2) the preservation of the grain size characteristics and structures of these soft sediments (Szcucinski 2012).

A first approach is to estimate the entrainment of fine sediments offshore based upon the simulated bed shear velocities of the tsunami waves (e.g., Maeno and Imamura 2007; Noda et al. 2007; Weiss 2008; Paris et al. 2010a). It is assumed that the flow generated by the tsunami is unidirectional, because the wave periods are very long, and that the predominantly sandy sediments behave in an essentially non-cohesive manner. The results illustrate the relationship between the critical threshold shear velocity of a specific grain size and the simulated tsunami shear velocity, thus giving estimates of the entrainment capability and maximum depth of sediment sources. It is particularly interesting to couple this approach with the determination of assemblages of marine fauna observed in tsunami deposits, such as foraminifera, diatoms or coccoliths. Uchida et al. (2010) suggested that foraminiferal tests are effective indicators of the source depth and transport distance of tsunami deposits. Surprisingly, Paris et al. (2010b) found no increase in open-ocean over coastal and shallow water taxa of nannoliths brought by the 2004 tsunami in Sumatra. In this case, the steep continental slope may have limited sediment transport upward from the Aceh basin (2,700–2,300 m deep) to the wide fore-arc shelf (depth <200 m).

Complete inverse models of flow from characteristics of tsunami deposits are still under development. The simple approach of Moore et al. (2007) and Smith et al. (2007) is based on the timescale taken for grains to settle out of suspension compared with the timescale of the wave. The model by Soulsby et al. (2007) relies on a simple trajectory-based theory of the tsunami hydrodynamics and sediment dynamics, and predicts the maximum inundation distance, wave height and velocity at the shore. The model assumes that there is a linear relationship between the decreasing mean grain size of the tsunami deposits and the increasing distance inland. Soulsby et al. (2007) agree that “the depth and velocity of a tsunami wave running up a sloping beach exhibit roughly parabolic and saw-tooth time-variations respectively, instead of the linear and constant-time variations respectively used in the simple theory,” and that (2) the grain size trends of sediments “responds to a balance of erosion, deposition and diffusion processes.”

Jaffe and Gelfenbaum (2007) proposed a model for calculating tsunami flow speed from the thickness and grain size distribution of tsunami sandy deposits. The model (TsuSed-Mod) assumes steady and uniform flow conditions, sediment fallout from suspension (normally graded deposits), and limited erosion during tsunami outflow (backwash). If units deposited as bedload are included, the model overestimates tsunami flow speed. TsuSedMod was applied to the deposits of the 1998 Papua New Guinea (Jaffe and Gelfenbaum 2007), 2004 Indian Ocean and 2006 Java tsunami (Spiske et al. 2010), and 2009 Samoa tsunami (Jaffe et al. 2011).

Pritchard and Dickinson (2008) investigated the transport of sediment both by suspension and bedload under different kinds of long non-breaking waves through a series of numerical experiments, considering the case of cross-shore flow over a uniform sloping beach. They demonstrate how the asymmetries between run-up and backwash contribute to net transport in the near-shore and beach zone, where tsunami deposits are rarely

preserved, due to fast post-tsunami reworking. Another limitation is that the effects of the topography on tsunami flow and related sedimentation are neglected (but finally it is not the aim of these numerical experiments).

2 Aim of the study

In this paper, we present the results of numerical simulations of the 2004 Indian Ocean earthquake and tsunami off the western coast of Sumatra, integrating sediment erosion and deposition. We investigate the transport of sediment both by suspension and by bedload under different kinds of long breaking dispersive waves through a series of numerical experiments, considering the case of in situ erosion and deposition of sediment related to run-up flow depth. Considering (1) the complexity of flow dynamics and influence of the micro-scale features (buildings, walls, slope breaks) on sediment transport and (2) the scarcity of direct observations of the 2004 tsunami in Lhok Nga, we remind that this study is not devoted to a realistic reproduction of a case study, but rather of methodological interest.

The study area is the Lhok Nga Bay (Fig. 1), a 5-km large embayment opened to the Indian Ocean. The coast is sandy, locally protected by fringing reefs. Low areas correspond to lagoons, swamps and rice crops. Small hills and hummocky terrains refer to dunes, beach ridges and paleodunes reaching 15 m a.s.l. (northern part of the bay). The “Tsunarisk” franco-indonesian project conducted by Franck Lavigne and Raphaël Paris previously published detailed reconstruction of the tsunami in Lhok Nga (Lavigne et al. 2009), description and interpretation of coastal erosion, boulder and sand deposition onshore and offshore (Paris et al. 2007, 2009, 2010a, b; Wassmer et al. 2007), and numerical modeling of boulder transport (Nandasena et al. 2011).

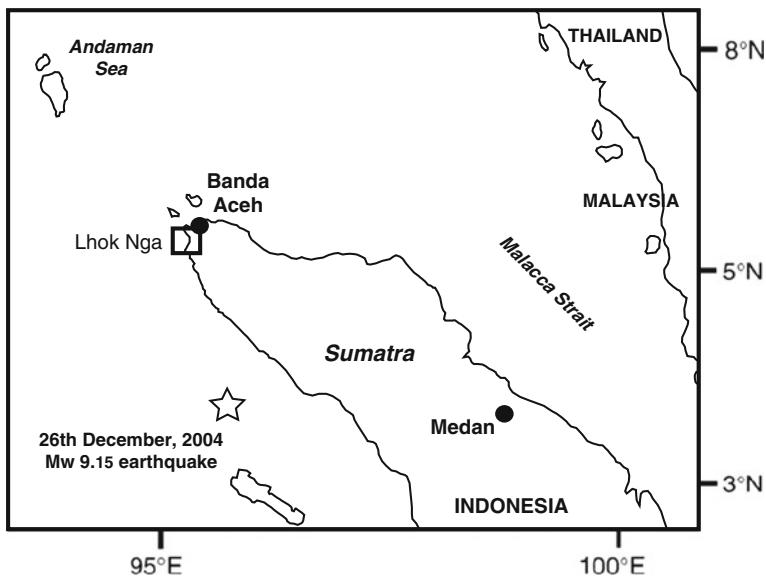


Fig. 1 Location map of the study area (Lhok Nga Bay, Sumatra, Indonesia) and December 26, 2004, earthquake epicenter

3 Methods

3.1 Sediment transport and deposition

The suspended and bedload transport formulas are coupled with the flow field, and the bedload ϕ is estimated through the formula of Ribberink (1998):

$$\phi = 11 * \sqrt{\left[\left(\frac{\rho_s - \rho_w}{\rho_w} \right) * g * d_{50}^3 \right]} * (\theta_c - \theta_{cr})^{1.65} \tag{1}$$

where θ is the Shields number, ρ_s is the sediment density, ρ_w is the seawater density, and d_{50} is the median grain size of the sediments. In Eq. 1, the bedload ϕ is related to the bedload sediment flux S_b by the following formula:

$$S_b = \phi \sqrt{\left(\frac{\rho_s - \rho_w}{\rho_w} \right) * g * d_{50}^3} \tag{2}$$

The suspended load is derived from the equation of conservation of mass for suspended sediment:

$$\frac{\partial C}{\partial t} + u \frac{\partial C}{\partial x} + v \frac{\partial C}{\partial y} + (w - w_s) \frac{\partial C}{\partial z} = \frac{\partial}{\partial x} \left[\frac{v_t}{\sigma_c} \frac{\partial C}{\partial x} \right] + \frac{\partial}{\partial y} \left[\frac{v_t}{\sigma_c} \frac{\partial C}{\partial y} \right] + \frac{\partial}{\partial z} \left[\frac{v_t}{\sigma_c} \frac{\partial C}{\partial z} \right] \tag{3}$$

where C is the suspended load concentration, w_s is the sediment settling velocity, and σ_c is the turbulent Schmidt number. The turbulent Eddy viscosity v_t is calculated using:

$$v_t = A \sqrt{[(d - d_{br}) u]^2 + [dw]^2} \tag{4}$$

where A is a coefficient (0.001), d is the total local water depth, d_{br} is total water depth at breaking, and u and w are horizontal and vertical velocity, respectively.

The boundary conditions for suspended sediment pickup and settling rate on the seabed are defined by the reference concentration formula of van Rijn (1984):

$$C_a = 0.015 \rho_s \frac{d_{50}(T_*)^{1.5}}{a(D_*)^{0.3}} \tag{5}$$

$$T_* = \frac{\tau_b - \tau_{cr}}{\tau_{cr}} \tag{6}$$

$$D_* = d_{50} \left[\frac{(s - 1)g}{v^2} \right]^{0.3} \tag{7}$$

$$a = k_s = \Delta/2 \tag{8}$$

where C_a is the sediment volume concentration, T_* is the dimensionless bed shear stress parameter, a is the bed roughness, D_* is the dimensionless particle parameter, τ_b is the bed shear stress, τ_{cr} is the critical shear stress, s is the relative density ($\rho_s - \rho_w$), v is the kinematic viscosity, k_s is the sediment grain roughness coefficient, and Δ is the median grain size of the sediments.

The bed morphology rate of change ($\delta Z_b/\delta t$) is defined by van Rijn (1984) formula as follows:

$$\rho_s(1 - p) \frac{\partial z_b}{\partial t} + D_a + E_a + \frac{\partial s_b}{\partial x} = 0 \tag{9}$$

where p is the porosity, Z_b is the bed level above datum, D_a is suspended sediment deposition rate, E_a is the suspended sediment erosion rate, S_b is bedload sediment flux, χ is the horizontal grid spacing in x and y direction. D_a and E_a are given by:

$$E_a = \frac{v_t}{\sigma_{s,z}} \frac{\partial C}{\partial t} \tag{10}$$

$$D_a = w_s C_a \tag{11}$$

Theoretically, sediment transport by short waves in the swash zone requires a special treatment (e.g., Larson and Wamsley 2007; Nam et al. 2009), which is not applied here, because we believe that it is not necessary for long tsunami waves.

3.2 Numerical simulations

The suspended sediment erosion–deposition rate and bedload sediment flux are coupled with the flow field obtained by COMCOT hydrodynamic code (Liu et al. 1998). The COMCOT code generates 2-D depth integrated dispersive wave flow field, and the near-bed suspended sediment concentration is estimated by the flow field and bottom shear stress relationship. COMCOT code solves shallow water equations. A numerical dispersion is introduced, in order to recover the dispersion relationship of Boussinesq equation. The turbulence effect of breaking waves on sediment suspension and concentration C_a is considered by adding the bottom shear stress and turbulent viscosity terms to the momentum equation, as expressed below:

$$u_{xt} + \nabla \eta + \frac{a_0}{h_0} (u_x \cdot \nabla) u_x + \left(\frac{h_0}{l}\right)^2 \left\{ \frac{z_x^2}{2} \nabla(\nabla \cdot u_{xt}) + z_x \nabla[\nabla \cdot (hu_{xt})] \right\} - \tau_b + v_t \nabla[\nabla \cdot (hu_{xt})] = 0 \tag{12}$$

The near-bed horizontal and upward velocities and pressure for the quasi three dimensions can be expressed in the following terms (Nwogo 1993):

$$w = -\left(\frac{h_0}{l}\right)^2 \nabla \cdot (hu_x) - \left(\frac{h_0}{l}\right)^2 z \nabla \cdot u_x + O(\mu^4) \tag{13}$$

A digital elevation model (DEM) was constructed using DGPS and echosounder, and completed by pre-tsunami satellite images, ortho-rectified aerial photographs and bathymetric charts (for a detailed explanation of the DEM construction, see Lavigne et al. 2006). Simulations were performed with a large 90-m grid including Banda Aceh (northern coast) and an 18-m grid focusing on Lhok Nga Bay (western coast), thus giving a nested grid ratio of 1/5. Simulations were run with the nonlinear shallow water equations. Linear shallow water equations are no longer valid for the continental shelf, since the wave amplitude/length ratio increases significantly (Liu et al. 1998). The results presented herein were obtained using the nonlinear dispersive breaking wave model. Bottom friction was included as a variable roughness coefficient, which was determined after field data both offshore and onshore (Lavigne et al. 2006; Paris et al. 2009, 2010a, b).

Different source scenarii for the 2004 earthquake were proposed from seismic and geodetic data (e.g., Ammon et al. 2005; Vigny et al. 2005; Subarya et al. 2006; Chlieh et al.

2007; Koshimura et al. 2008). It is not the aim of this paper to discuss the reliability of these different source models and the regional distribution of tsunami run-ups, which have been widely discussed (e.g., Choi et al. 2006; Tanioka et al. 2006; Grilli et al. 2007; Kowalik et al. 2007; Rabinovich and Thomson 2007; Ioualalen 2009; Prasetya et al. 2011). Our major concern is not to find the source model which best accounts for all observed run-ups all along the Indian Ocean coasts, but only for the tsunami inundation observed in the Lhok Nga Bay (Fig. 2) and described in detail by Lavigne et al. (2009). Several models of fault segments were tested: Ammon et al. (2005), Subarya et al. (2006) and Koshimura et al. (2008).

4 Results and discussion

4.1 Earthquake source models and tsunami run-ups

In Lhok Nga, the tsunami wave heights ranged from 20 to 30 m at the coast, with local run-ups exceeding 50 m a.s.l. (Lavigne et al. 2009). Figure 2 displays the isoflood map deduced from the field measurements of flow depths (modified from Lavigne et al. 2009).

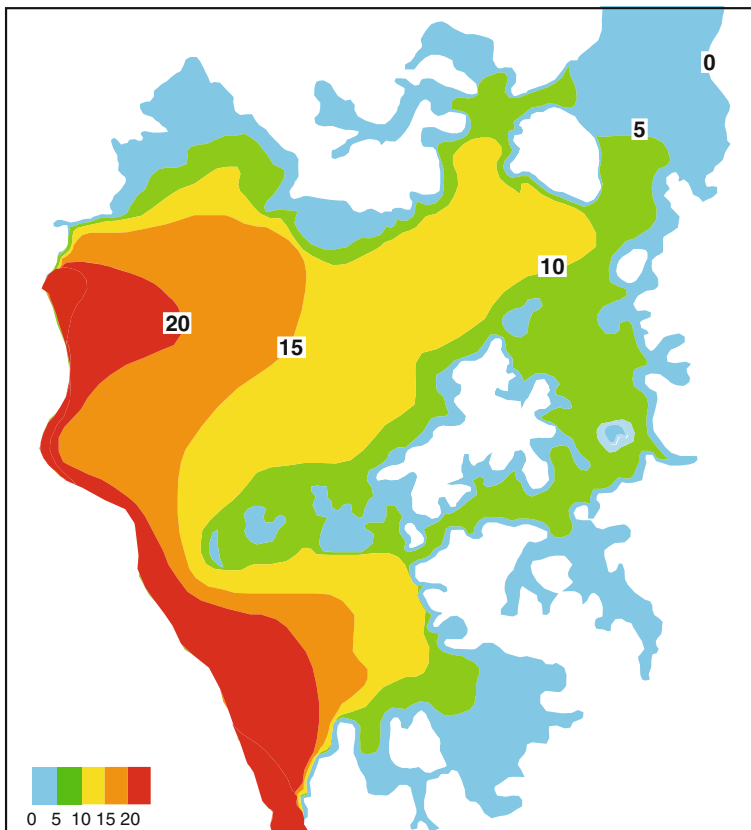


Fig. 2 Tsunami isoflood map of Lhok Nga Bay, after field data (modified from Lavigne et al. 2009)

The earthquake source model used by Koshimura et al. (2008) with a 25-m dislocation better reproduces the wave travel time, flow depth and inundation area than the other models tested (Figs. 3 and 4). All models fail reproducing the highest run-ups observed and flow depths higher than 20 m near the coast, even with a 30-m dislocation which clearly overestimates the flow depth more inland (Fig. 5). The discrepancies between the simulation and the field data may come from (1) the influence of the increasing amount of debris on wave’s propagation landward, (2) the local effect of anthropic infrastructures (e.g., buildings, dams) which are not reproduced by the DEM, and (3) also the fact that measured depths often represent minimum values (see discussion in Lavigne et al. 2009). The results presented in the following sections were obtained with the 25-m dislocation scenario after 150 min of simulation.

4.2 Coastal erosion

Both tsunami inflow and outflow produced extensive erosion, sediment transport and deposition up to 5 km inland (Umitsu et al. 2007; Paris et al. 2009). The erosional imprints of the tsunami extend to 500 m from the shoreline and exceed 2 km along the river beds. The most eroded coasts were tangent to the tsunami wave train, which came from the southwest. The fringing reefs were not efficient in reducing erosion and destruction inland (Baird et al. 2005). The geomorphological impact of the tsunami was evidenced by beach and dune erosion, destruction of sand barriers protecting the lagoons or at river mouths, numerous erosion escarpments of soils, bank erosion in the river beds, dislodgement of clasts from cliffs and coral reefs.

We only present the final balance of erosion and deposition after 150 min of simulations in order to compare with the measures of coastal erosion and thickness of tsunami deposits measured after the tsunami (Paris et al. 2009). We could present a timing of the simulated processes of erosion and deposition, such as filling of inflow erosional features by the outflow, but without any validation by field data which only represent the final result. Our model fairly predicts the pronounced coastal retreat in the northern part of Lhok Nga Bay (Fig. 6), where coastal segments are tangent to the tsunami wave train coming from the Southwest. Paris et al. (2009) estimated a mean coastal retreat of 80 m in this area (Lampuuk and fringing reef), with values ranging between 40 and 200 m (calculations made each 100 m of shoreline). The simulation gives coastal retreats between 50 and 150 m. In terms of area, there is a good agreement between the simulation (195,400 m²) and the field (203,200 m²). In the golf area, the simulation greatly overestimates coastal

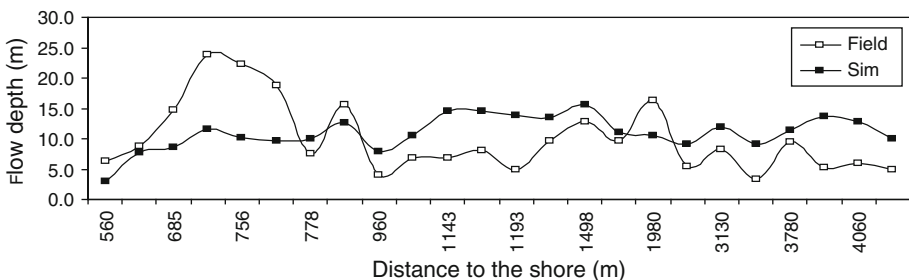


Fig. 3 Comparisons between the simulated maximum flow depth (25-m dislocation) and measured minimum flow depth (Lavigne et al. 2009). The 24 ground control points are listed from 430 to 5,600 m inland

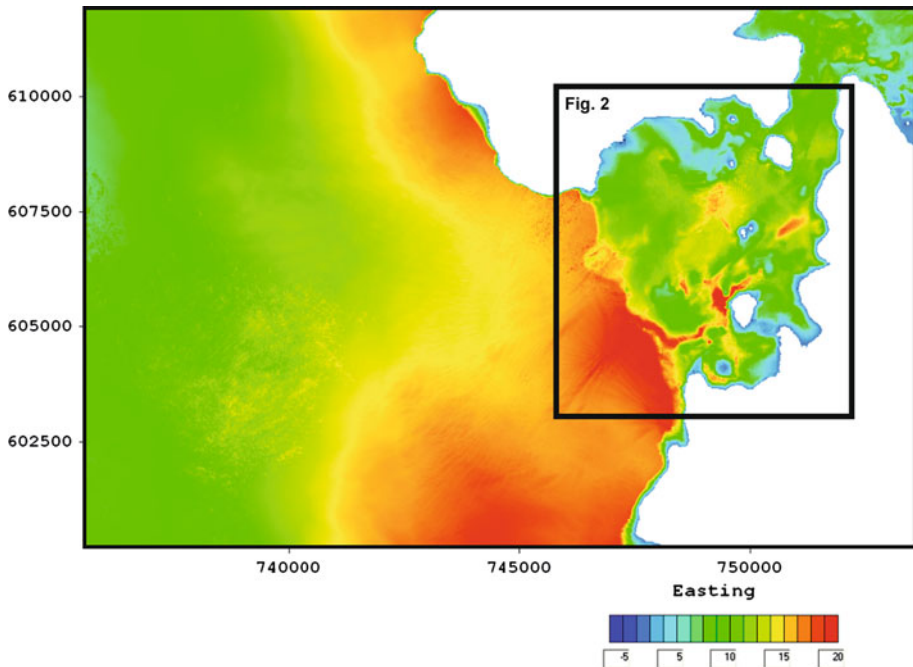


Fig. 4 Simulated maximum flow depth (m) with a source dislocation of 25 m (source model from Koshimura et al. 2008)

retreat ($23,500 \text{ m}^2/5,300 \text{ m}^2$ measured). South of the Lhok Nga River (Fig. 6), a coseismic land subsidence up to 2 m was measured (Paris et al. 2009), thus complicating the comparison between the simulation and the field data. The simulation cannot reproduce the significant reduction in coastal retreat by the boulder dam of the Lafarge residence (Fig. 6), because the available DEM does not include this dam. In the model, the coastal erosion zone does not display incision channels created by the outflow, as described by Fagherazzi and Du (2008) in Indonesia and Thailand.

4.3 Sediment deposition

The 2004 tsunami carried a large amount of sediments and debris. Eyewitness accounts recall waves already black before breaking inland (Lavigne et al. 2009). Characteristics of tsunami deposits in Lhok Nga Bay were previously described by Moore et al. (2006) and Paris et al. (2007). Paris et al. (2009) estimated that the total volume of sediments left inland by the tsunami between Lampuuk and the Lhok Nga River ranged between $500,000$ and $1,500,000 \text{ m}^3$ (this is a rough estimate calculated after measurements of deposits thickness on a 100-m grid). This result suggests that the simulation may underestimate tsunami deposition ($611,700 \text{ m}^3$). Fig. 6 illustrates the sensitivity of the erosion/deposition model to the topography, as confirmed by field observations (e.g., Umitu et al. 2007; Fagherazzi and Du 2008; Paris et al. 2009) and suggested by experimental studies (e.g., Apotsos et al. 2011). Compared with a 20-m tsunami wave front, even small-scale features such as walls, roads, trenches or rice paddies may affect flow dynamics and related sediment transport and deposition.

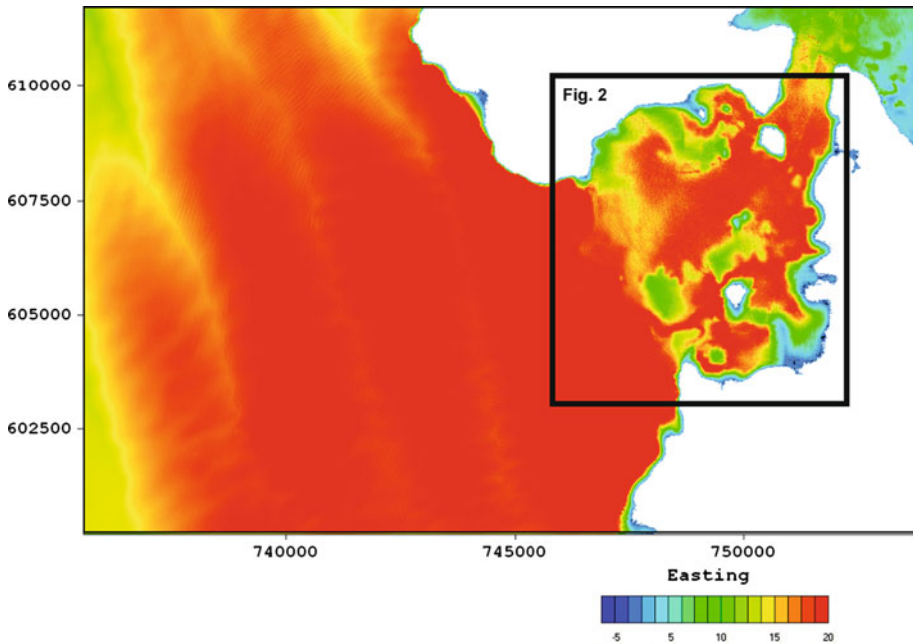


Fig. 5 Simulated maximum flow depth (m) with a source dislocation of 30 m (source model from Koshimura et al. 2008)

The model fully reproduces the observed thickness of tsunami deposits when considering both bedload and suspension (Fig. 7). The discrepancies are due to inaccuracies and resolution of the DEM. For instance, some small gullies, buildings or levees between rice paddies are not represented on an 18-m grid even if they may impact the spatial distribution of the deposition. When bedload only is considered, the model slightly underestimates the thickness of deposits (Fig. 8), especially in the flat bottom central area of the bay (e.g., rice paddies located between 1.5 and 2.5 km inland). Thus, bedload dominates, but a significant amount of sediment is transported in suspension, as previously discussed (e.g., Gelfenbaum and Jaffe 2003; Nanayama and Shigeno 2006; Paris et al. 2007; Choowong et al. 2008; Jaffe et al. 2011).

Several authors suggested that the 2004 tsunami backwash (outflow) have reworked and redeposited significant volumes of sediments in the river beds and offshore (Feldens et al. 2009; Paris et al. 2010a, Nandasena et al. 2011). The deposition/erosion balance is mostly positive in the Lhok Nga River and offshore zone (Fig. 6), except on the rocky slopes of the fringing reef (where the model is no longer available).

5 Conclusions

Coupling the bedload and suspended transport with the hydrodynamic model of tsunami propagation and inundation inland is a promising tool, as demonstrated by the methodology proposed in this study. Nevertheless, developing models of sediment transport and deposition by tsunami is still confronted with two limitations: (1) the model of tsunami inundation inland must fit reasonably the observed flow depth and velocity, (2) the bedload

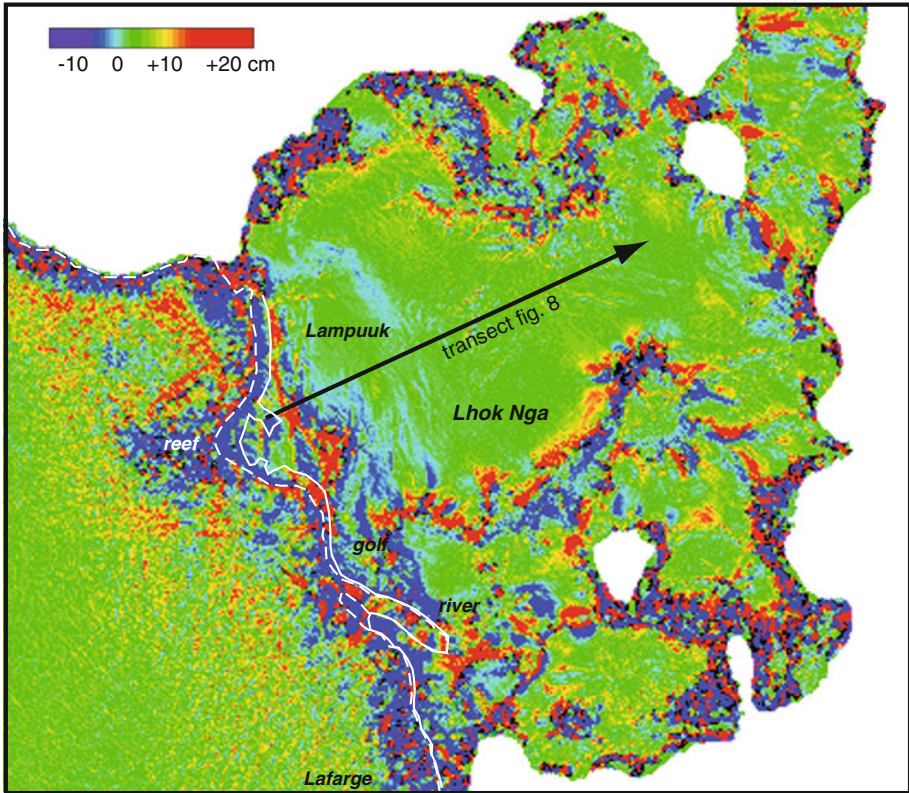


Fig. 6 Map of total erosion and sediment deposition in the Lhok Nga Bay after 150 min of simulation (25 m dislocation model). The *white lines* represent the pre-tsunami (Ikonos January 2003) and post-tsunami (Ikonos December 2004) coastlines (Paris et al. 2009)

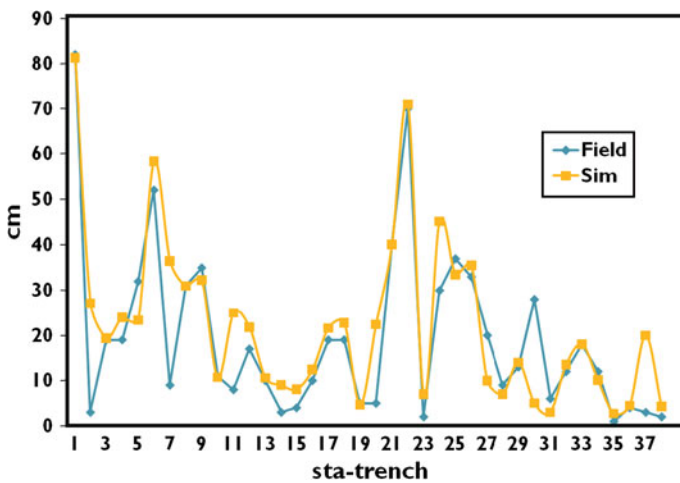


Fig. 7 Comparison between simulated (this study) and observed (Paris et al. 2009) thickness of tsunami deposits (m) for 38 stations sorted by their distance to the shoreline (increasing from *left to right*)

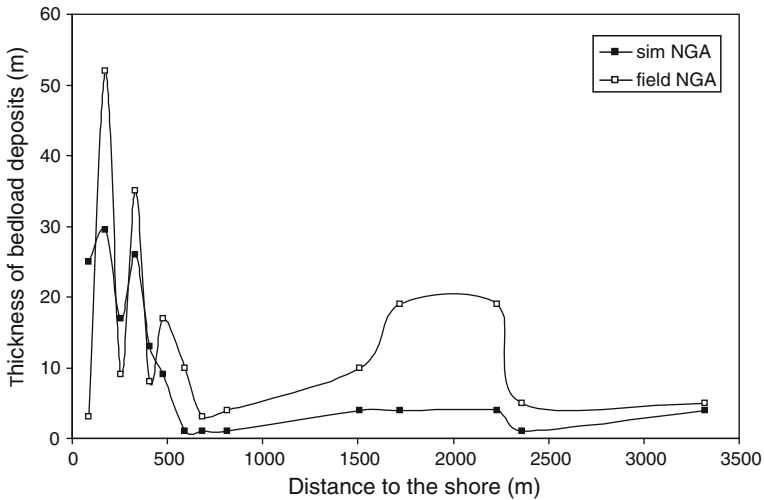


Fig. 8 Comparison between simulated (this study) and observed (Paris et al. 2007) thickness of bedload deposits (m) along a *longitudinal* transect from the coast (*left*) to 3.3 km inland (*right*)

transport is influenced by micro-scale topographic or anthropic features which are not always reproduced by the DEM, and (3) the increasing amount of debris as the wave propagates landward may influence flow dynamics (Prasetya et al. 2012). Further improvements would represent an important step toward the tsunami inverse model from the deposits to the source.

Another questioning issue in the applicability of inverse models to paleotsunami research is the preservation of tsunami deposits, especially under tropical climate (high seasonal rainfall), in coastal lowlands (bioturbation) and in densely occupied areas (surface reworking). Szczucinski (2012) reinvestigated the 2004 tsunami deposits along the Andaman coast of Thailand four years after the tsunami. He found that in about 50 % of the sites, the deposits were not preserved. The deposits preserved were eroded, and their internal structure was blurred, thus modifying any grain-size trend (e.g., upward and landward fining). Szczucinski (2012) concludes that “modelling of paleotsunami parameters that are based on paleorecords must take into account the post-depositional changes (particularly related to soil’s formation) since the model’s input parameters (thickness, grain size) are subjected to modifications.”

Acknowledgments This work was funded by French ANR (*Agence Nationale de la Recherche*) program Risknat—project Maremoti (2008–2012) whose leader is H el ene H ebert (CEA-DASE). The authors are particularly grateful to two anonymous reviewers for their relevant comments. This is Laboratory of Excellence *ClerVolc* contribution n o 39.

References

- Ammon CJ, Ji C, Thio HK, Robinson D, Ni S, Hjorleifsdottir V, Kanamori H, Lay T, Das S, Helmberger D, Ichinose G, Polet J, Wald D (2005) Rupture process of the 2004 Sumatra–Andaman earthquake. *Science* 308:1133–1139
- Aptosos A, Gelfenbaum G, Jaffe B (2011) Wave characteristics and morphologic effects on the onshore hydrodynamic response of tsunamis. *Coast Eng* 58:1034–1048

- Chlieh M, Avouac J, Hjorleifsdottir V, Song TA, Ji C, Sieh K, Sladen A, Hébert H, Prawirodirdjo L, Bock Y, Galetzka J (2007) Coseismic slip and afterslip of the great Mw 9.15 Sumatra-Andaman earthquake of 2004. *Bull Seismol Soc Am* 97:S152–S173
- Choi BH, Hong SJ, Pelinovsky E (2006) Distribution of runup heights of the December 26, 2004 tsunami in the Indian Ocean. *Geophys Res Lett* 33(13):L13601
- Choowong M, Murakoshi N, Hisada K, Charoentitirat T, Charusiri P, Phantuwongraj S, Wongkok P, Choowong A, Subsajun R, Chutakositkanon V, Jankaew K, Kanjanapayont P (2008) Flow conditions of the 2004 Indian Ocean tsunami in Thailand, inferred from capping bedforms and sedimentary structures. *Terra Nova* 20:141–149
- Fagherazzi S, Du X (2008) Tsunamigenic incisions produced by the December 2004 earthquake along the coasts of Thailand, Indonesia and Sri Lanka. *Geomorphology* 99:120–129
- Feldens P, Schwarzer K, Szczucinski W, Stattegger K, Sakuna D, Somgpongchaiykul P (2009) Impact of the 2004 Indian Ocean tsunami on seafloor morphology and sediments offshore Pakarang Cape, Thailand. *Pol J Environ Stud* 18(1):63–68
- Gelfenbaum G, Jaffe B (2003) Erosion and sedimentation from the 17 July, 1998 Papua New Guinea tsunami. *Pure Appl Geophys* 160:1969–1999
- Grilli ST, Ioualalan M, Asavanant J, Shi F, Kirby J, Watts P (2007) Source constraints and model simulation of the December 26, 2004, Indian Ocean tsunami. *J Waterw Port Coast Ocean Eng* 133:414–429
- Ioualalan M (2009) Sensitivity tests on relations between tsunami signal and seismic rupture characteristics: the 26 December 2004 Indian Ocean event case study. *Environ Model Softw* 24(12):1354–1362
- Jaffe B, Gelfenbaum G (2007) A simple model for calculating tsunami flow speed from tsunami deposits. *Sediment Geol* 200:347–361
- Jaffe B, Buckley M, Richmond B, Strotz L, Etienne S, Clark K, Watt S, Gelfenbaum G, Goff J (2011) Flow speed estimated by inverse modeling of sandy sediment deposited by the 29 September 2009 tsunami near Satitua, east Upolu, Samoa. *Earth Sci Rev* 107:23–37
- Koshimura S, Oie T, Yanagisawa H, Imamura F (2008) Developing fragility functions for tsunami damage estimation using numerical model and post-tsunami data from Banda Aceh, Indonesia. *Coast Eng J* 51(3):243–273
- Kowalik Z, Knight W, Logan T, Whitmore P (2007) The tsunami of 26 December, 2004: numerical modeling and energy considerations. *Pure Appl Geophys* 164:379–393
- Larson M, Wamsley TV (2007) A formula for longshore sediment transport in the swash. *Proceedings Coast Sed'07, ASCE, New Orleans: 1924–1937*
- Lavigne F, Paris R, Wassmer P, Gomez C, Brunstein D, Grancher D, Vautier F, Sartohadi J, Setiawan A, Gunawan T, Waluyo B, Fachrizal, Mardiatno D, Widagdo A, Cahyadi R, Lespinasse N, Mahieu L (2006) Learning from a major disaster (Banda Aceh, December 26th, 2004): a methodology to calibrate simulation codes for tsunami inundation models. *Zeitschrift für Geomorphol Suppl Band* 146:253–265
- Lavigne F, Paris R, Grancher D, Wassmer P, Brunstein D, Vautier F, Leone F, Flohic F, De Coster B, Gunawan T, Gomez Ch, Setiawan A, Cahyadi R, Fachrizal (2009) Reconstruction of tsunami inland propagation on December 26, 2004 in Banda Aceh, Indonesia, through field investigations. *Pure Appl Geophys* 166:259–281
- Liu PL-F, Woo SB, Cho YS (1998) Computer programs for tsunami propagation and inundation. Technical report, Cornell University
- Maeno F, Imamura F (2007) Numerical investigations of tsunamis generated by pyroclastic flows from the Kikai caldera, Japan. *Geophys Res Lett* 34:L23303
- Moore A, Nishimura Y, Gelfenbaum G, Kamataki T, Triyono R (2006) Sedimentary deposits of the 26 December 2004 tsunami on the northwest coast of Aceh, Indonesia. *Earth Planet Space* 58:253–258
- Moore A, McAdoo B, Ruffman A (2007) Landward fining from multiple sources in sand sheet deposited by the 1929 grand banks tsunami, Newfoundland. *Sediment Geol* 200(3–4):336–346
- Morton RA, Goff JR, Nichol SL (2008) Hydrodynamic implications of textural trends in sand deposits of the 2004 tsunami in Sri Lanka. *Sediment Geol* 207(1–4):56–64
- Nam PT, Larson M, Hanson H, Hoan LX (2009) A numerical model of nearshore waves, currents, and sediment transport. *Coast Eng* 56:1084–1096
- Nanayama F, Shigeno K (2006) Inflow and outflow facies from the 1993 tsunami in southwest Hokkaido. *Sediment Geol* 187:139–158
- Nandasena NAK, Paris R, Tanaka N (2011) Numerical assessment of boulder transport by 2004 Indian Ocean tsunami in Lhok Nga, West Banda Aceh (Sumatra, Indonesia). *Comput Geosci* 37:1391–1399
- Noda A, Katayama H, Sagayama T, Suga K, Uchida Y, Satake K, Abe K, Okamura Y (2007) Evaluation of tsunami impacts on shallow marine sediments: an example from the tsunami caused by the 2003 Tokachi-oki earthquake, Northern Japan. *Sediment Geol* 200:314–327

- Nwogu O (1993) An alternative form of the Boussinesq equations for nearshore wave propagation. *J Waterw Port Coast Ocean Eng* 199:618–638
- Paris R, Lavigne F, Wassmer P, Sartohadi J (2007) Coastal sedimentation associated with the December 26, 2004 in Lhok Nga, west Banda Aceh (Sumatra, Indonesia). *Mar Geol* 238:93–106
- Paris R, Wassmer P, Sartohadi J, Lavigne F, Barthomeuf B, Desgages É, Grancher D, Baumert Ph, Vautier F, Brunstein D, Gomez Ch (2009) Tsunamis as geomorphic crisis: lessons from the December 26, 2004 tsunami in Lhok Nga, west Banda Aceh (Sumatra, Indonesia). *Geomorphology* 104:59–72
- Paris R, Fournier J, Poizot E, Etienne S, Morin J, Lavigne F, Wassmer P (2010a) Boulder and fine sediment transport and deposition by the 2004 tsunami in Lhok Nga (western Banda Aceh, Sumatra, Indonesia): a coupled offshore—onshore model. *Mar Geol* 268:43–54
- Paris R, Cachao M, Fournier J, Voldoire O (2010b) Nannoliths abundance and distribution in tsunami deposits: example from the December 26, 2004 tsunami Lhok Nga (northwest Sumatra, Indonesia). *Geomorphol Relief Process Environ* 2010(1):109–118
- Prasetya G, Borrero J, de Lange W, Black K, Healy T (2011) Modeling of inundation dynamics on Banda Aceh, Indonesia during the great Sumatra tsunamis December 26, 2004. *Nat Hazards* 58:1029–1055
- Prasetya G, Black K, de Lange W, Borrero J, Healy T (2012) Debris dispersal modeling for the great Sumatra tsunamis on Banda Aceh and surrounding waters. *Nat Hazards* 60:1167–1188
- Pritchard D, Dickinson L (2008) Modelling the sedimentary signature of long waves on coasts: implications for tsunami reconstruction. *Sed Geol* 206:42–57
- Rabinovich AB, Thomson RE (2007) The 26 December 2004 Sumatra Tsunami: analysis of tide gauge data from the World Ocean part 1 Indian Ocean and South Africa. *Pure Appl Geophys* 164:261–308
- Ribberink JS (1998) Bed-load transport for steady flows and unsteady oscillatory flows. *Coast Eng* 34:59–82
- Smith DE, Foster IDL, Long D, Shi S (2007) Reconstructing the pattern and depth of flow onshore in a paleotsunami from associated deposits. *Sediment Geol* 200(3–4):362–371
- Soulsby RL, Smith DE, Ruffman A (2007) Reconstructing tsunami run-up from sedimentary characteristics—a simple mathematical model. Sixth International Symposium on Coastal Processes—coastal sediments'07 coasts, Oceans, Ports and River Institute (COPRI) of the American Society of Civil Engineers, May 13–17, New Orleans, Louisiana Vol. 2, pp 1075–1088
- Spiske M, Weiss R, Bahlburg H, Roskosch J, Amijaya H (2010) The TsuSedMod inversion model applied to the deposits of the 2004 Sumatra and 2006 Java tsunami and implications for estimating flow parameters of palaeo-tsunami. *Sediment Geol* 224:29–37
- Subarya C, Chlieh M, Prawirodirdjo L, Avouac J-P, Bock Y, Sieh K, Meltzner AJ, Natawidjaja DH, McCaffrey R (2006) Plate boundary deformation associated with the great Sumatra—Andaman earthquake. *Nature* 440:46–51
- Szczuciński W (2012) The post-depositional changes of the onshore 2004 tsunami deposits on the Andaman Sea coast of Thailand. *Nat Hazards* 60:115–133
- Tanioka Y, Kasusose T, Kathirolu S, Nishimura Y, Iwasaki S, Satake K (2006) Rupture process of the 2004 great Sumatra—Andaman earthquake estimated from tsunami waveforms. *Earth Planet Space* 58:203–209
- Uchida JI, Fujiwara O, Hasegawa S, Kamataki T (2010) Sources and depositional processes of tsunami deposits: analysis using foraminiferal tests and hydrodynamic verification. *Island Arc* 19:427–442
- Umitsu M, Tanavud C, Patanakanog B (2007) Effects of landforms on tsunami flow in the plains of Banda Aceh, Indonesia, and Nam Khem, Thailand. *Mar Geol* 242:141–153
- van Rijn LC (1984) Sediment transport Part II: suspended load transport. *J Hydraul Eng* 110(11):1613–1641
- Vigny C, Simons WJF, Abu S, Bamphenyu R, Satirapod C, Choosakul N, Subarya C, Socquet A, Omar K, Abidin HZ, Ambrosius BAC (2005) Insight into the 2004 Sumatra—Andaman earthquake from GPS measurements in southeast Asia. *Nature* 436:201–206
- Weiss R (2008) Sediment grains moved by passing tsunami waves: tsunami deposits in deep water. *Mar Geol* 250(3–4):251–257